

# Supplementary Materials

## Supplementary Figures and Tables

---

### 3D chromatin conformation correlates with replication timing and is conserved in resting cells

Benoit Moindrot<sup>1</sup>, Benjamin Audit<sup>2</sup>, Petra Klous<sup>3</sup>, Antoine Baker<sup>2</sup>, Claude Thermes<sup>4</sup>, Wouter de Laat<sup>3</sup>, Philippe Bouvet<sup>1</sup>, Fabien Mongelard<sup>1</sup> and Alain Arneodo<sup>2\*</sup>

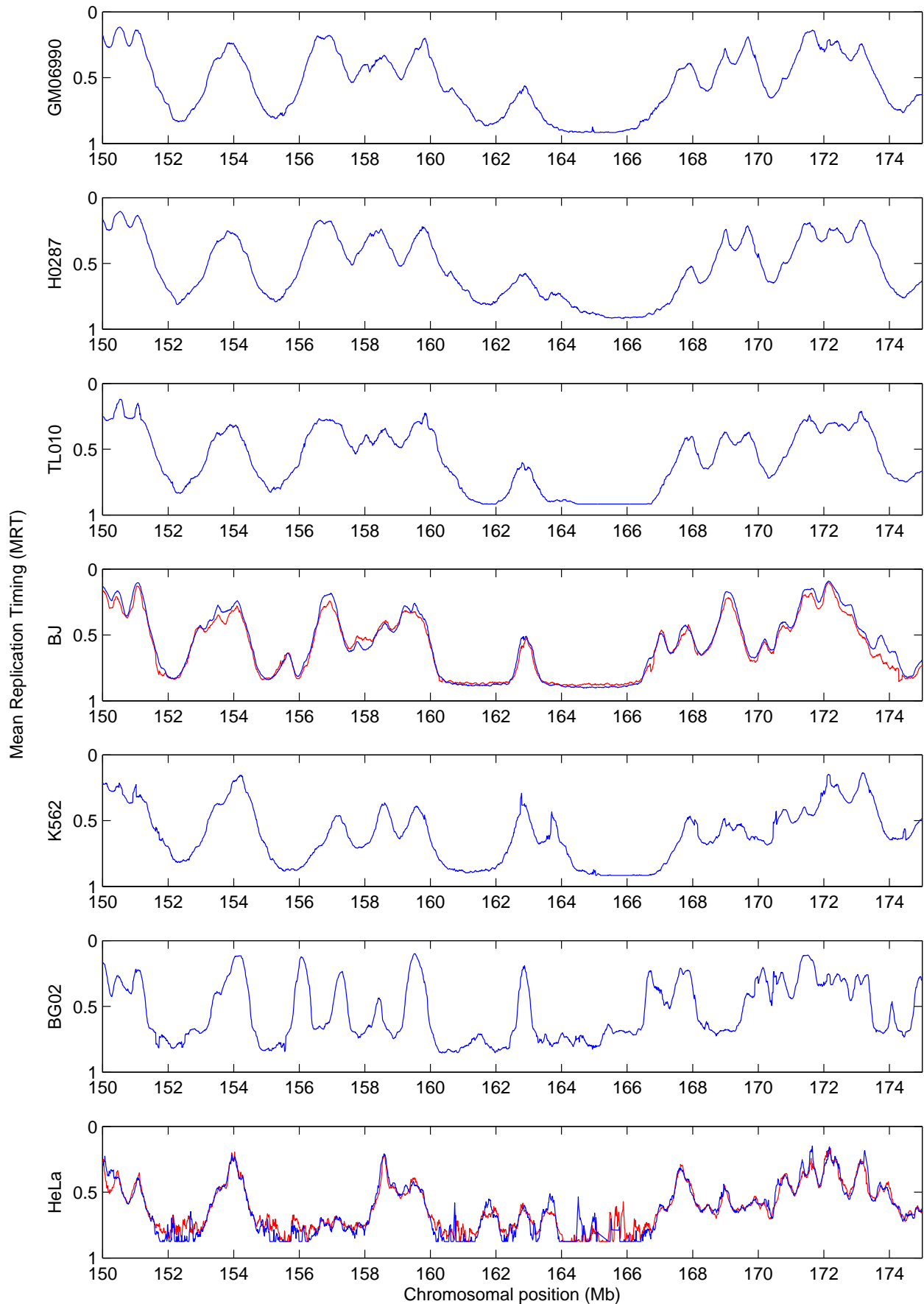
<sup>1</sup> Laboratoire Joliot-Curie, Ecole Normale Supérieure de Lyon, CNRS, F-69007 Lyon, France ; Université de Lyon, F-69000 Lyon, France

<sup>2</sup> Laboratoire de Physique, Ecole Normale Supérieure de Lyon, CNRS, F-69007 Lyon, France ; Université de Lyon, F-69000 Lyon, France

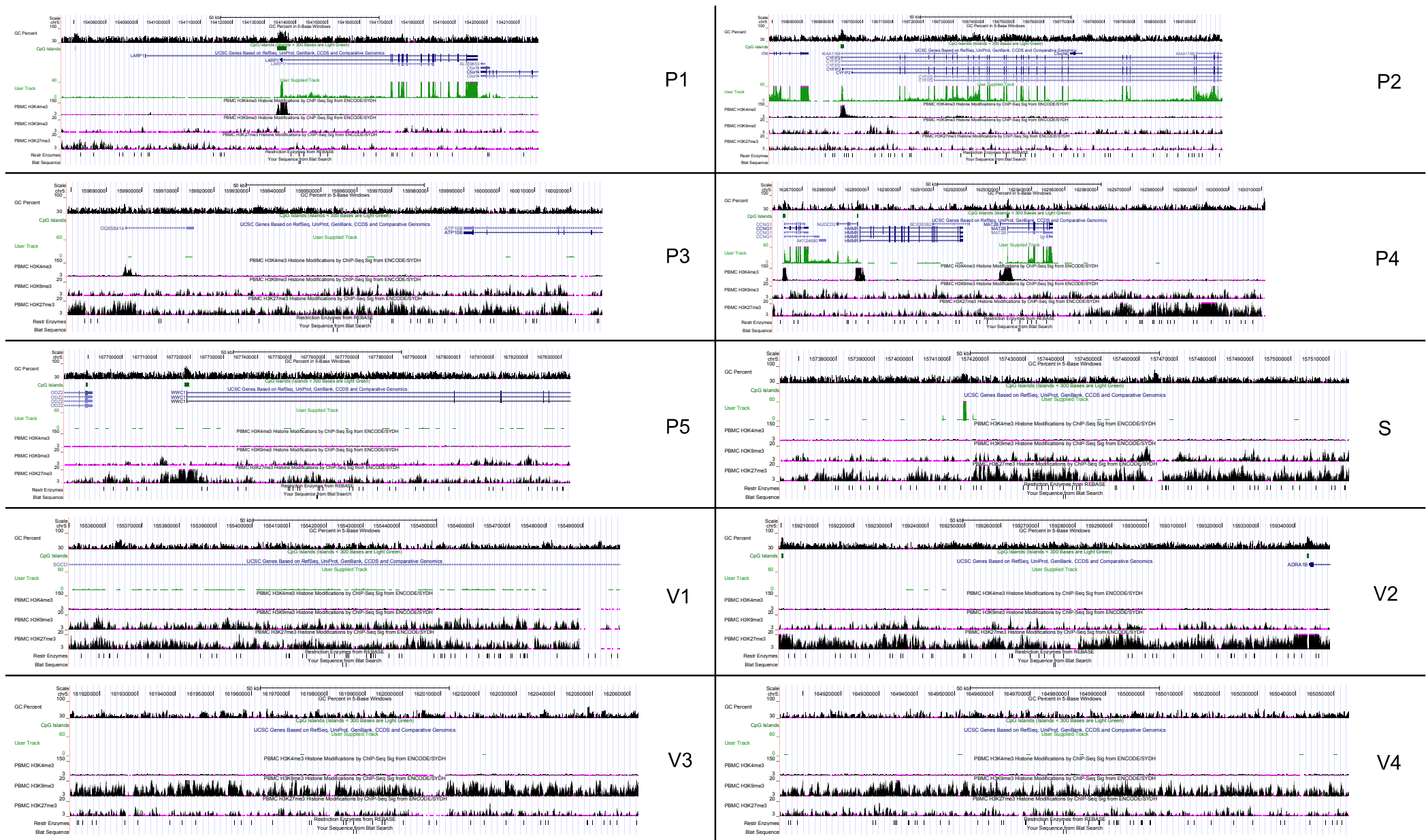
<sup>3</sup> Centre de Génétique Moléculaire (CNRS UPR3404), Allée de la Terrasse, 91198 Gif-sur-Yvette, France

<sup>4</sup> Hubrecht Institute-KNAW & University Medical Center Utrecht, Uppsalalaan 8, 3584 CT Utrecht, The Netherlands

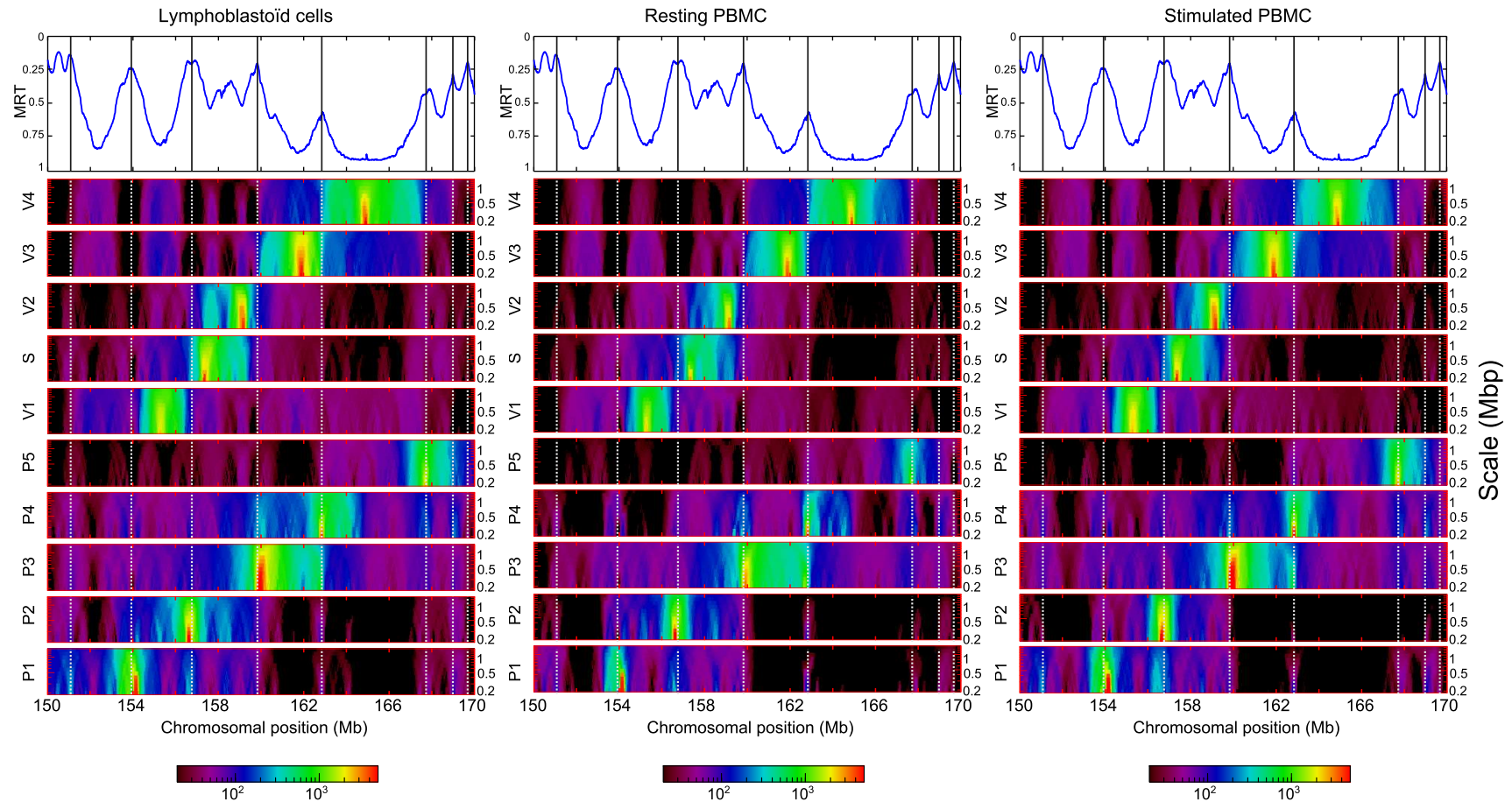
\* Corresponding author : Email : [alain.arneodo@ens-lyon.fr](mailto:alain.arneodo@ens-lyon.fr)



**Supplementary Figure S1: Replication timing of the 150-175 Mb portion of human chromosome 5 in different cell types.** From top to bottom, Replication timing of lymphoblastoids cells (Gm06990, H0287), lymphoblastoids with fragile X syndrome (TL010), normal fibroblasts (BJ, two replicates), a chronic myelogenous leukemia cell line with erythroid properties (K562), a human embryonic stem cell line (BG02), and HeLa cell line (two replicates). These replication timing data were retrieved from (1) and (2). For y-axis, zero value indicates an early replicated locus, and 1 value a late replicated one.



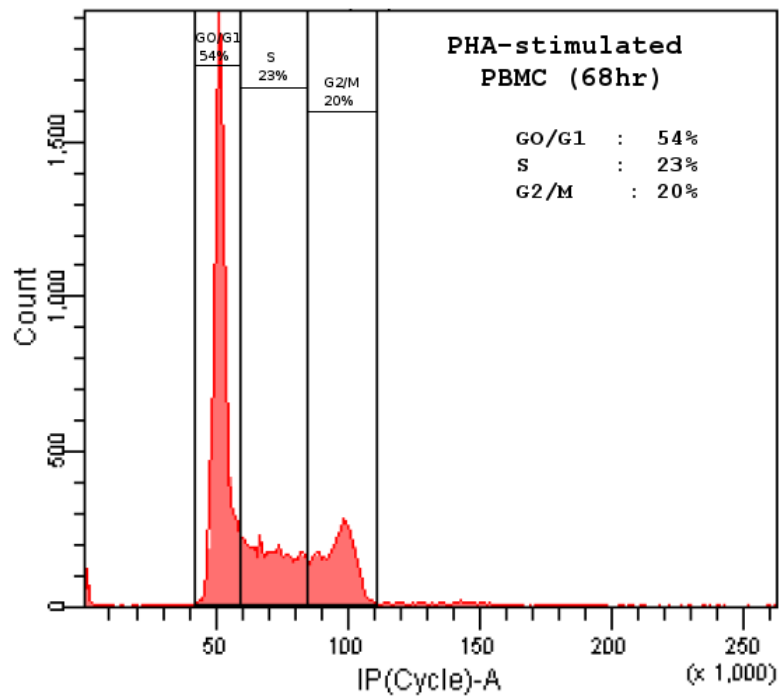
**Supplementary Figure S2: Local chromatin properties around the ten selected viewpoints in PBMC.** Using the UCSC genome-browser, we analyzed in PBMC the local chromatin properties in 150kb intervals around selected viewpoints. From the top to the bottom: the GC content (5bp window, hg19\_gc5Base); the presence of CpG island (hg19\_cpgIslandExt); the UCSC genes (hg19\_knownGene), mRNA expression in PBMC cells (display as user supplied track, GEO GSM669616); histones modifications in PBMC (H3K4me3 wgEncodeSydhHistonePbmcH3k04me3bUcdSig, H3K9me3 wgEncodeSydhHistonePbmcH3k09me3bUcdSig, and H3K27me3 wgEncodeSydhHistonePbmcH3k27me3bUcdSig); the HindIII restriction sites. The last track corresponds to the location of the two 4C-Seq primers. While 4C mapping was performed on the hg18 human assembly, these UCSC genome browser outputs correspond to the hg19 assembly in which chromatin data are available for PBMC cells. Lift-over tool was used to adapt 4C primers coordinates.



**Supplementary Figure S3: Space-scale representation of the 4C interaction frequencies of the 10 viewpoints in lymphoblastoid cells, resting PBMC and stimulated PBMC.** Each horizontal line corresponds to the median value of the interaction frequency computed in sliding windows of size ranging from 200 kb to 1.35 Mb. Due to the very large median-value dynamics, a logarithmic colormap was used (bottom).

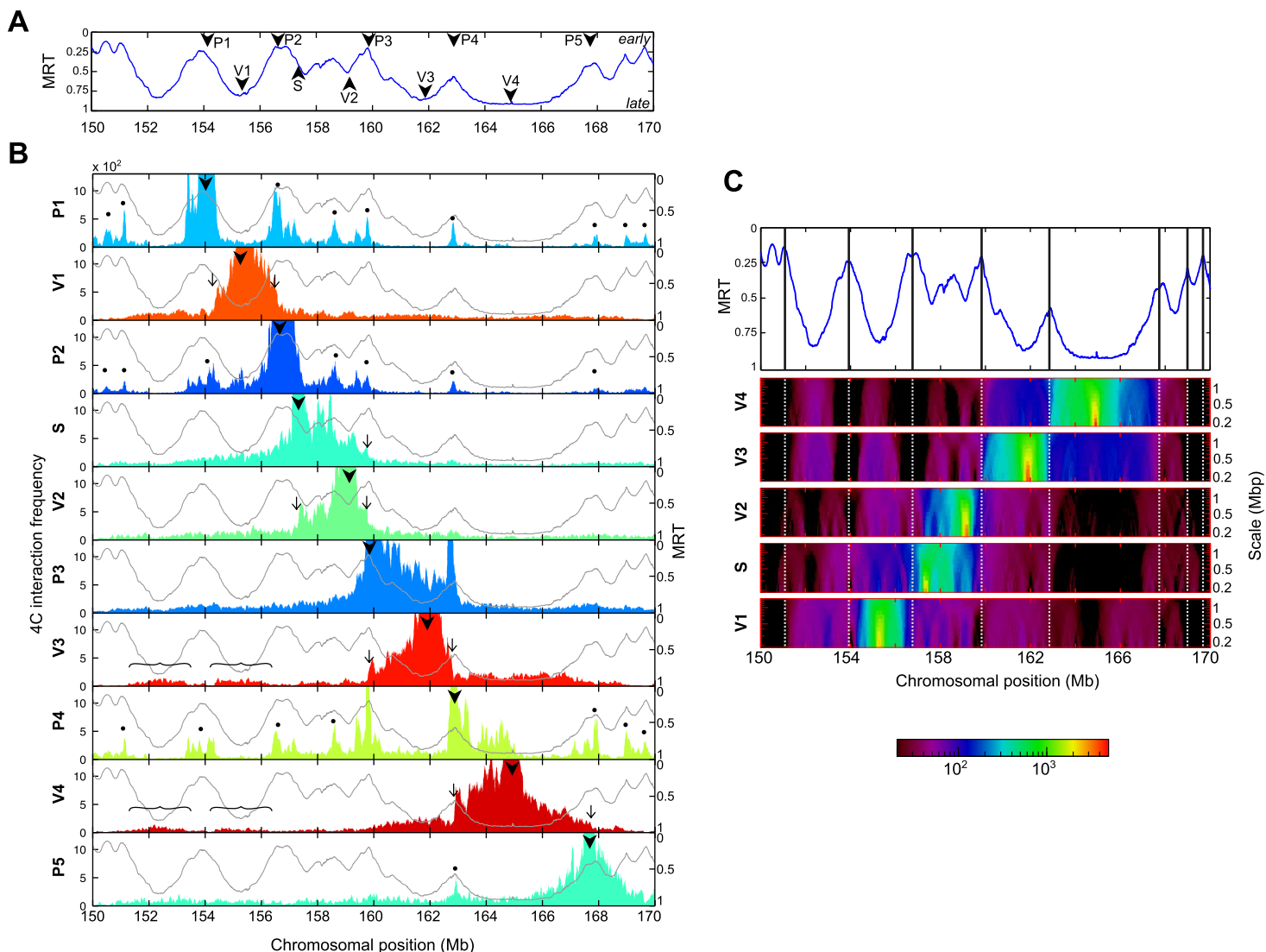
With S- and V-viewpoints, sharp transitions in the 4C signal occur at timing peaks. The 4C signals spread over the whole replication domain delineated by the timing peaks. A domain begins where the previous one ends : the 5'-transition from V4 viewpoint coincides with the 3'-transition from V3 viewpoint.

With P-viewpoints, similar sharp transitions are also observed within timing valleys, but unlike for S- and V-viewpoints, they do not coincide (for instance, the 3'-transition from P1 do not coincide with the 5'-transition from P2 transitions). This indicates that P-viewpoints do not define contiguous structural domains.



**Supplementary Figure S4: DNA content of 68hr PHA-stimulated PBMC.** An aliquot of PHA-stimulated PBMC used in 4C experiments was prepared for PI/FACS analysis. DNA content of cells was analyzed using FACSDiva™. The percentage of cells in G0/G1, S and G2/M is shown. Compared to resting cells, 40% of the cells are in S or G2/M phase after a 68hr-PHA treatment, and another fraction is probably also cycling through G1, albeit not detected in our analysis. This attests for an efficient cell-cycle entry.

## Resting PBMC



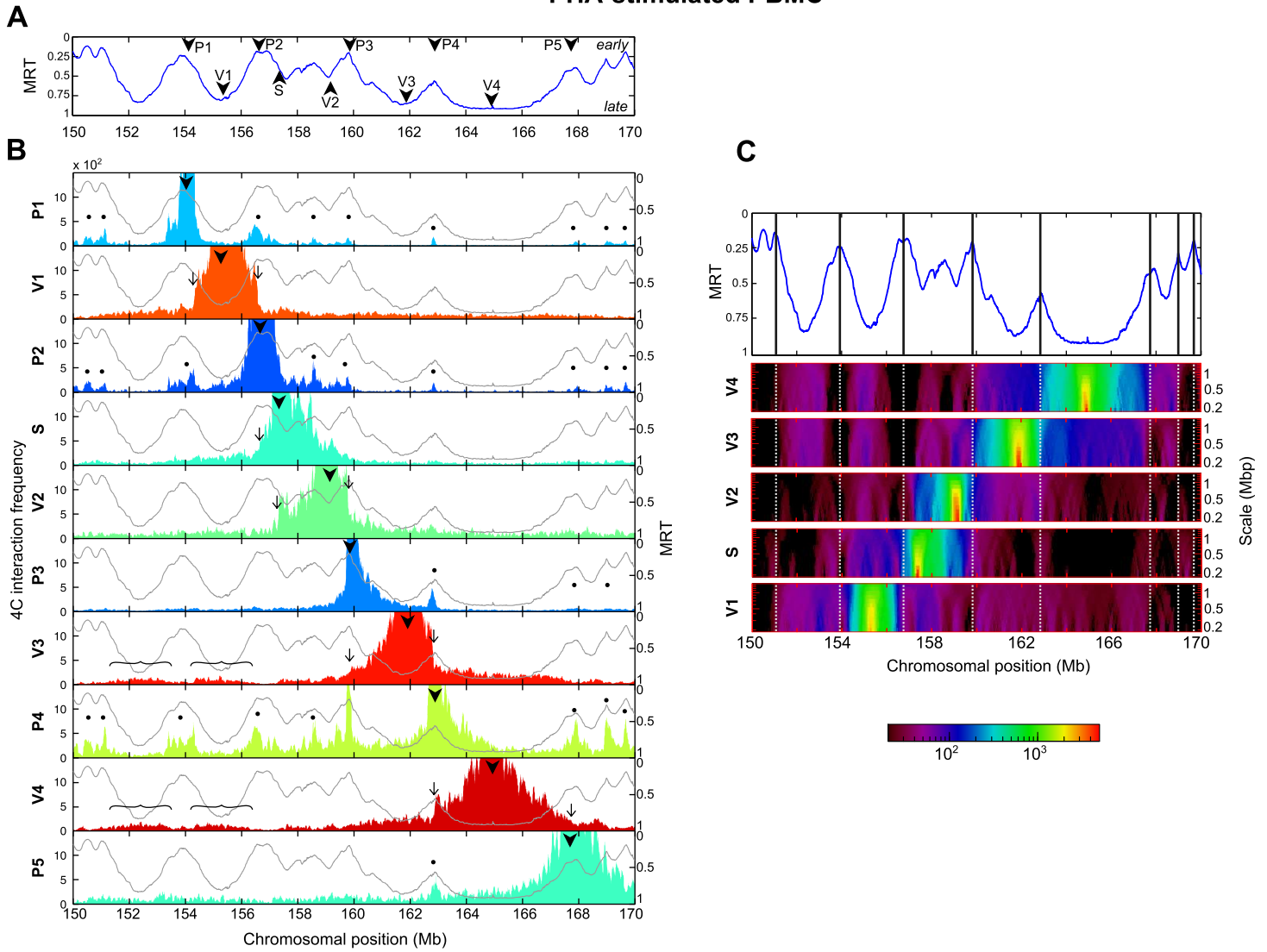
### Supplementary Figure S5: Local interaction properties in resting PBMC cells.

**A-** Mean replication timing (MRT) of the lymphoblastoid cell line Gm06990 in the portion 150-170 Mb of human chromosome 5 (1). Early-replicated sequences correspond to MRT values 0, whereas late replicated sequences correspond to MRT values ~1. The arrowheads indicate the position of the viewpoints used for the 4C analysis. Note that the y-axis of 4C profiles cannot be directly compared from one cell type to another if the total number of reads (Supplementary Table S3) is not similar.

**B-** Interaction frequency of the ten viewpoints in resting PBMC. Similar plots and analyses than in Figure 1B (main text). For each panel, the light grey curve corresponds to the replication timing and the colored filled curve to the 4C interaction frequency profiles. The arrowheads indicate the position of the viewpoints; the thin arrows indicate sharp drops in interaction frequency coinciding with timing peaks; the brackets indicate low-frequency small amplitude wave observed for V3 and V4 viewpoints; and the dots indicate preferential partners of P viewpoints coinciding with timing peaks.

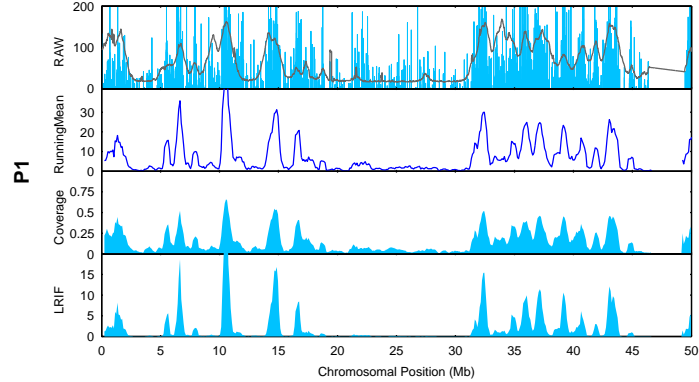
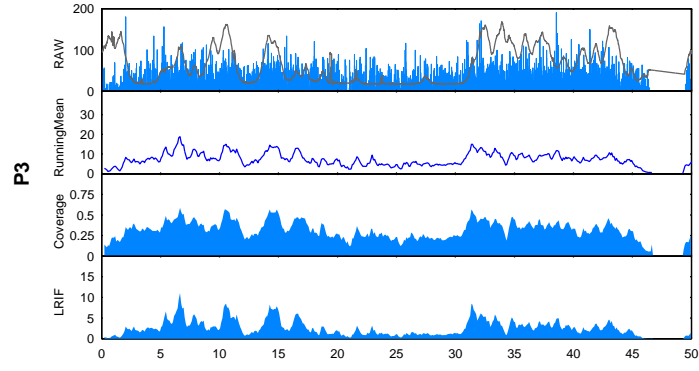
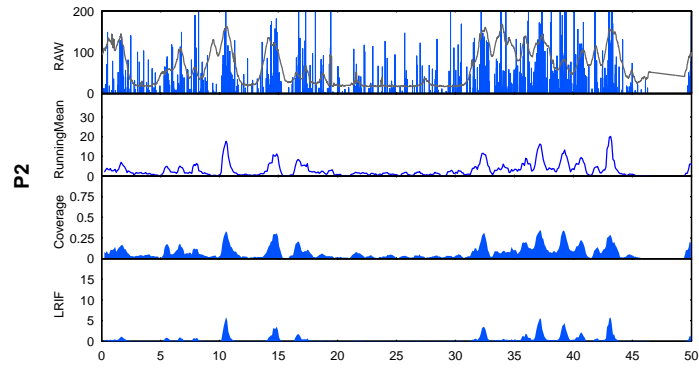
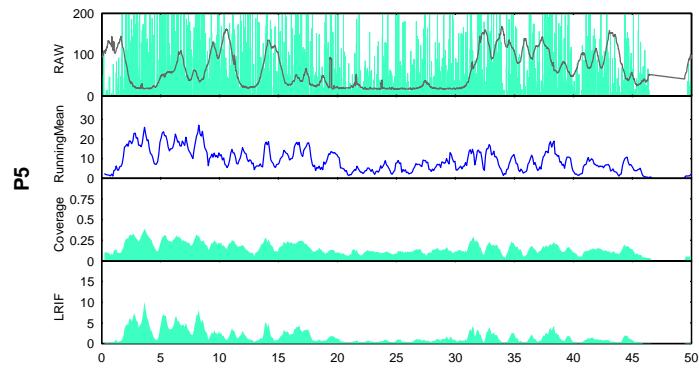
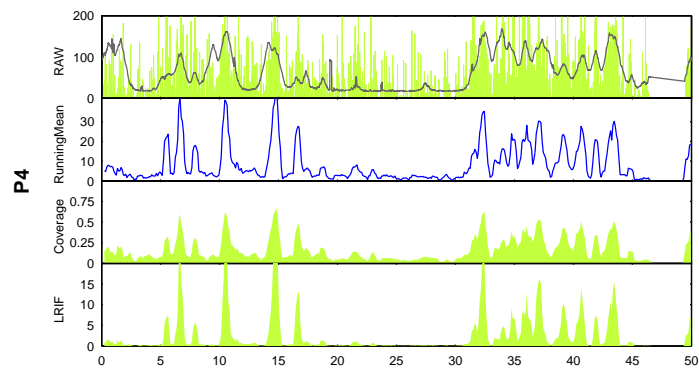
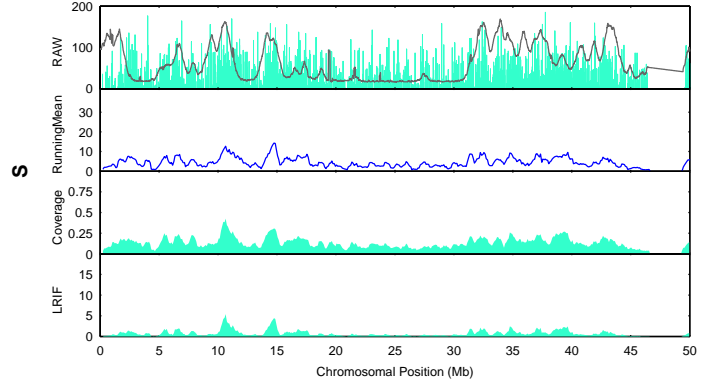
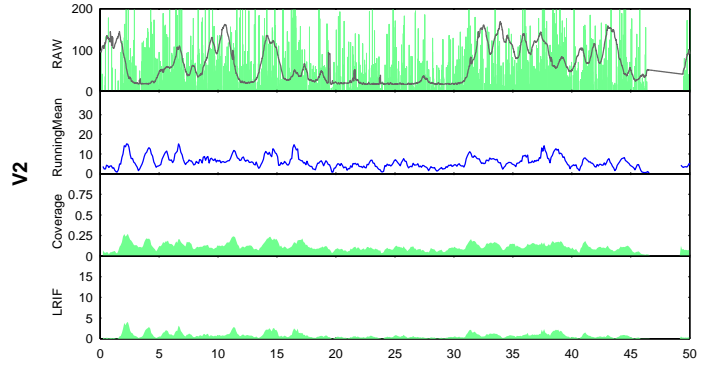
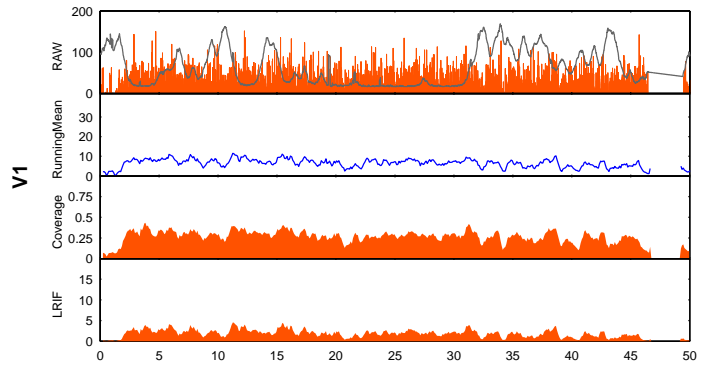
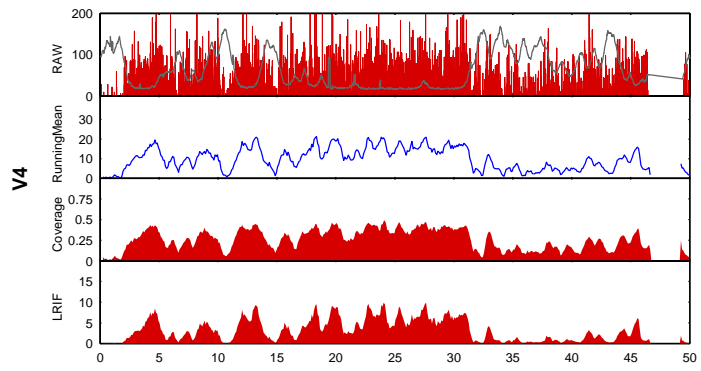
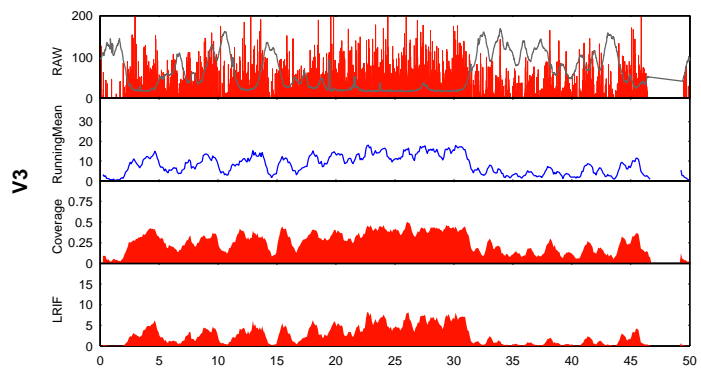
**C-** Timing peaks correspond to zones of sharp changes in 4C data interaction frequency. (Top) The position of timing peaks are marked along the MRT profile (vertical bars). (Middle) space-scale representation of the 4C interaction frequencies in resting PBMC for the viewpoints located in the 4 replication timing valleys (V1,V2,V3,V4) and in the replication timing transition region (S). Each horizontal line corresponds to the median value of the interaction frequency computed in sliding windows of size ranging from 200kb to 1.35Mb. Due to the very large median-value dynamics, a logarithmic colormap was used (bottom).

PHA-stimulated PBMC



**Supplementary Figure S6: Local interaction properties in PHA-stimulated PBMC cells.** Same as in Supplementary Figure S4 but with 68hr-PHA-stimulated PBMC.

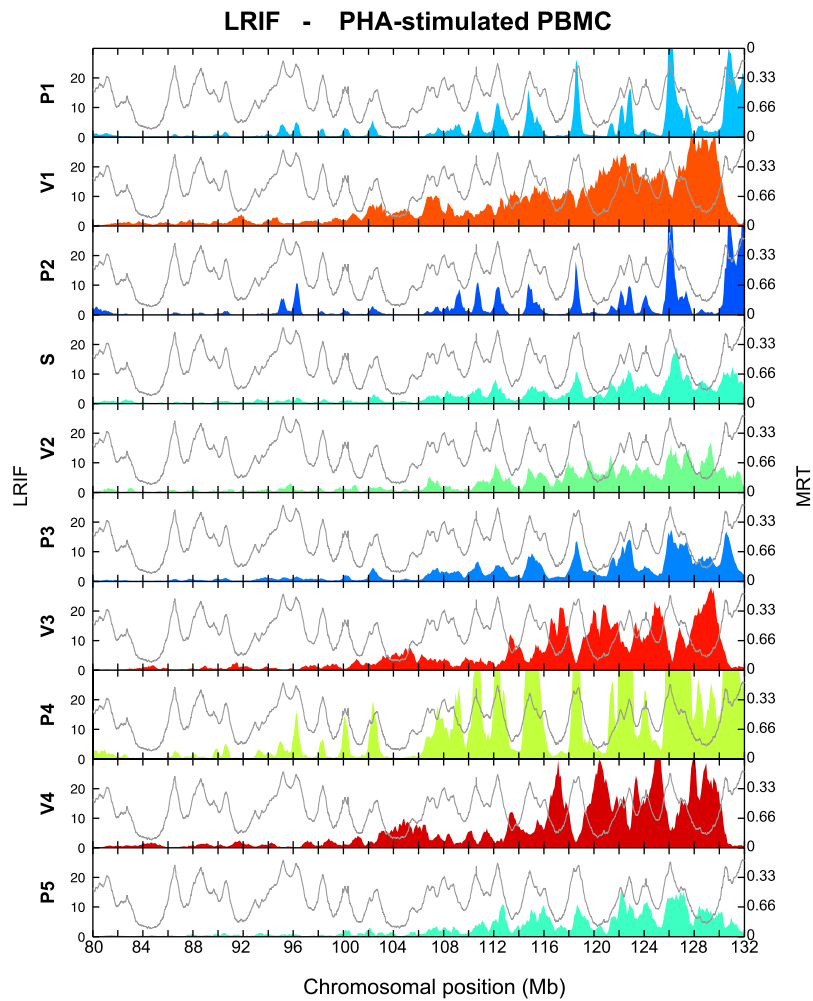




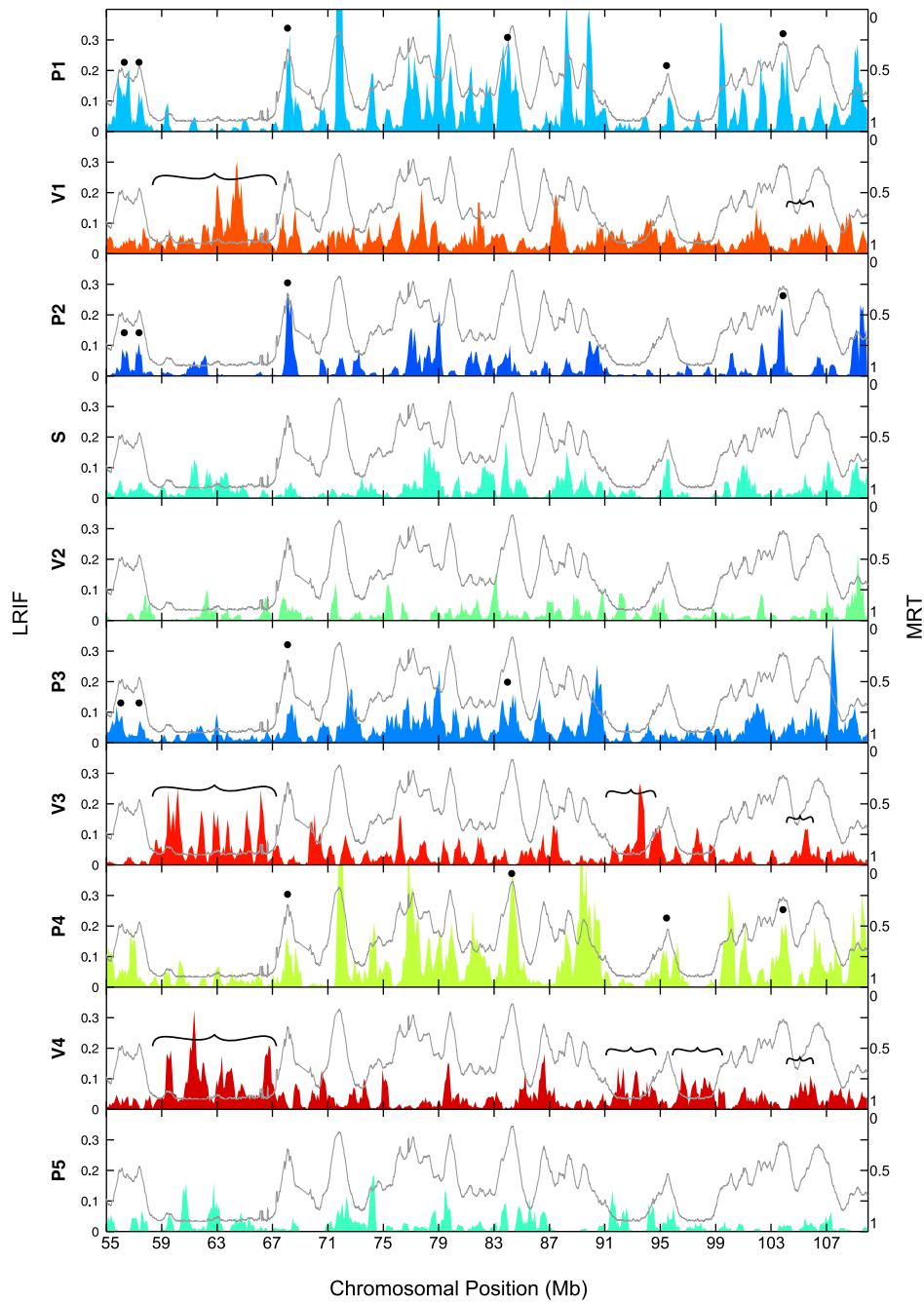


**Supplementary Figure S7: The detection of long-range interactions is independent on the variable choices.**

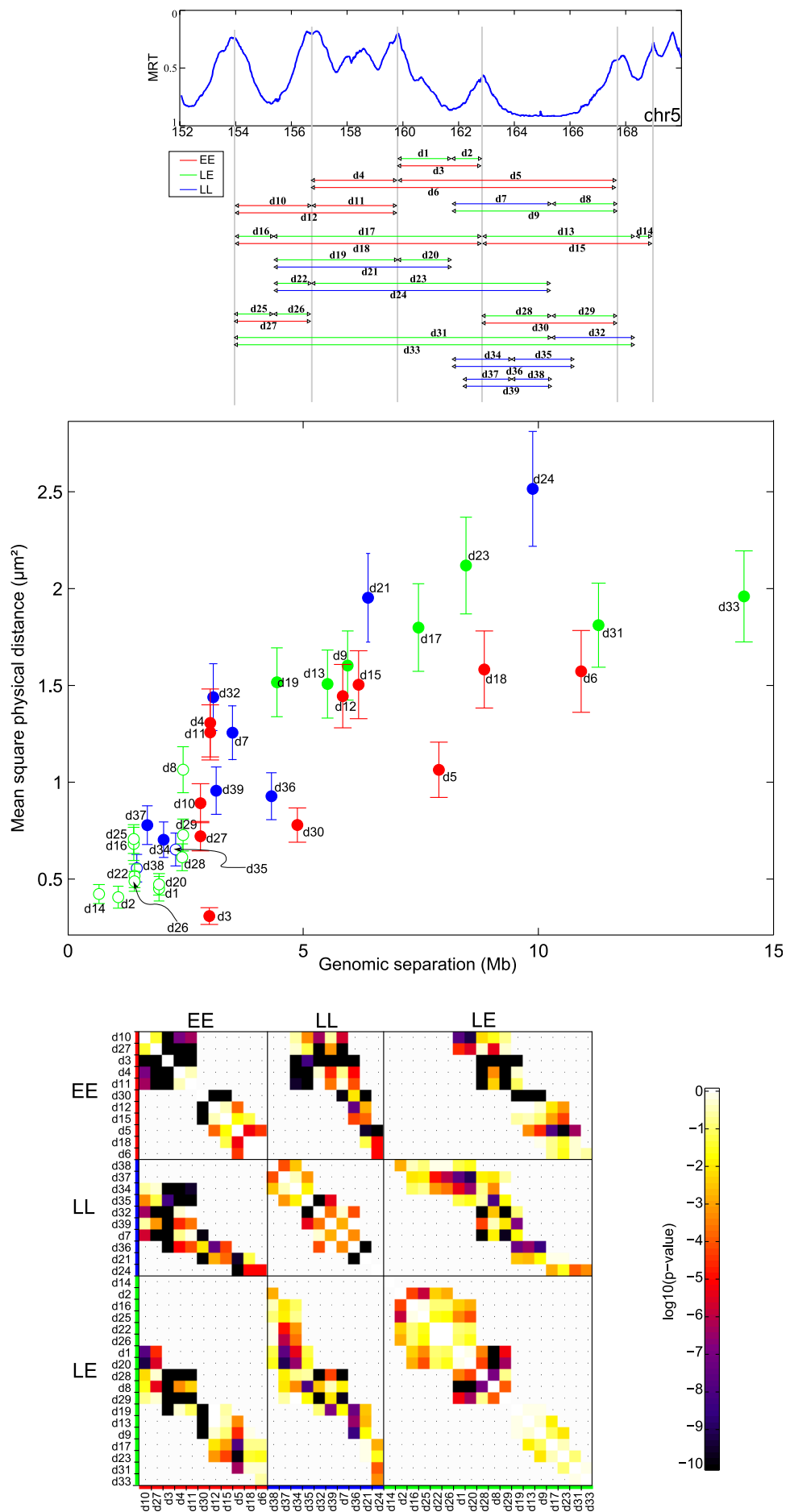
Since long-range interactions are rare events in a 4C library, we defined three different variables counting interaction events in a running window of size of 500 kb. The three different variables are shown for resting PBMC in the first 60Mb of human chromosome 5. These three variables display synchronized maxima and thus highlight similar long-range interactions. From top to bottom: (1) the RAW signal. Each bar corresponds to the number of reads per restriction fragment. The light grey curve corresponds to the replication timing (2) The Running Mean of the RAW signal on all the HindIII restriction sites of the genome. This running mean was calculated in a sliding window of 500 kb. At each step, the window slides of 100kb. (3) The coverage. We measured the percentage of HindIII restriction sites covered by reads. If a strong interaction exists, most of the restriction sites of the interacting partner should be covered by reads. Close to the viewpoints, the coverage is 1; farther away the coverage oscillates between 0 and 1. This value should reinforce the importance of the rare ligation events (few reads) concentrated on a small portion of chromatin. (4) To distinguish the case of concentrated ligation events with few reads from those with large read numbers, we defined a Long-Range Interaction Frequency (LRIF) variable corresponding to the product Coverage x Mean in a sliding window of 500 kb. This variable exhibits a large contrast signal:noise facilitating the detection of maxima (and thus of long-range interactions).



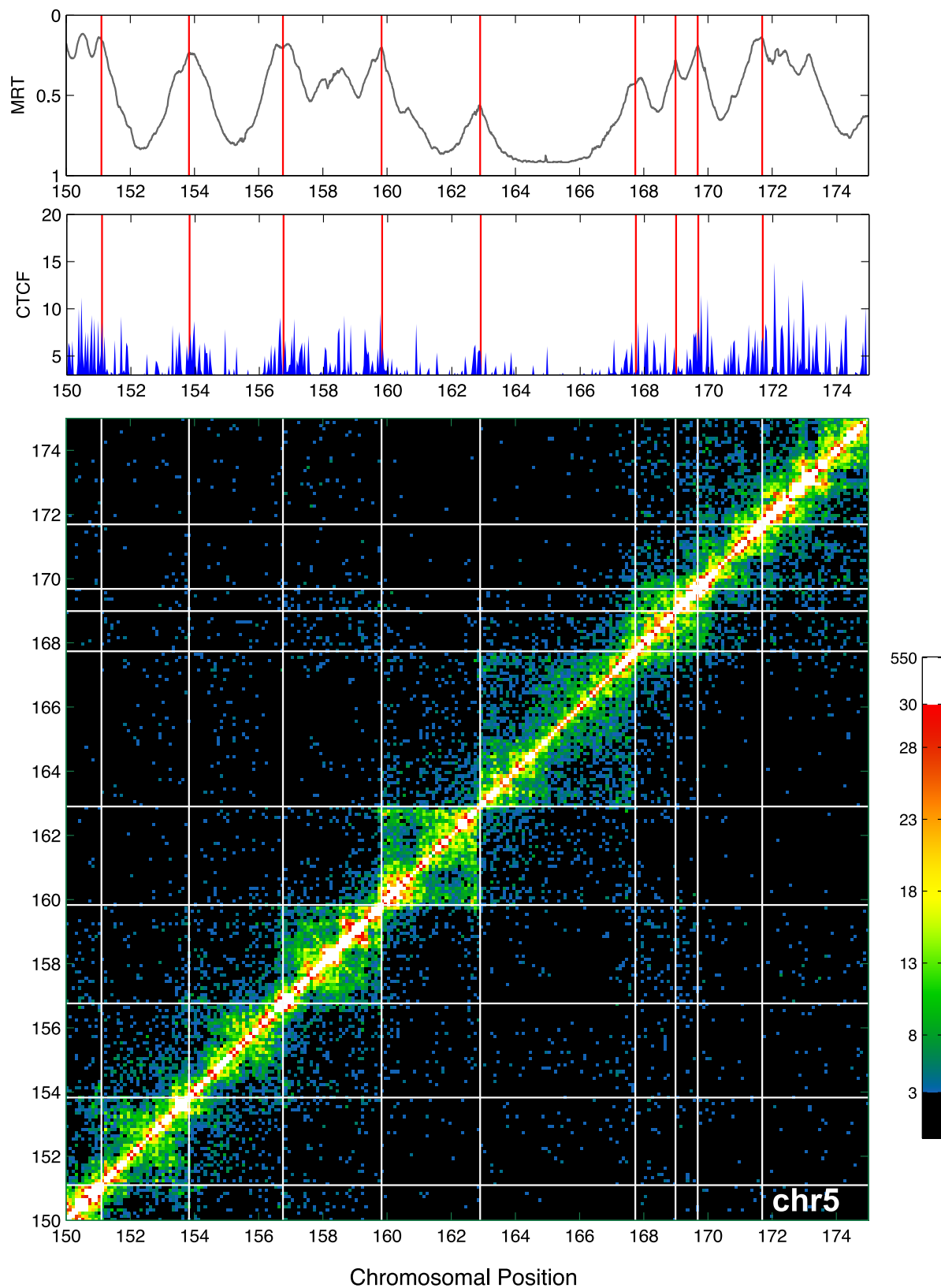
**Supplementary Figure S8: LRIF signals in PHA-stimulated PBMC.** LRIF values in 68hr-stimulated PBMC for the ten viewpoints (see Text and Materials and methods for the definitions). The colored filled curves correspond to the 4C profiles and the light grey curves correspond to the replication timing.



**Supplementary Figure S9: Inter-chromosomal LRIF signals in resting PBMC.** Long-range interaction frequency (LRIF) in resting PBMC for the ten viewpoints over 55 Mb of the human chromosome 4. The colored filled curves correspond to the 4C profiles and the light grey curves correspond to the replication timing. Note that, as compared to Fig. 2B, the LRIF y-axis has been considerably rescaled by a factor 100 to allow the visualization of small LRIF fluctuations. Even when considering different chromosomes, the late-replicating V1/V3/V4 viewpoints mostly interact with other late-replicated loci (brackets), whereas the early ones (P1, P2, P3, P4) contact other early timing peaks (dots).



**Supplementary Figure S10: FISH measured distances and pairwise statistics.** **Top :** Same as main Figure 4A. **Middle :** Same as main Figure 4E but with all labels. **Bottom :** Pairwise t-test with an alpha risk = 0.5. Pairwise statistical tests were performed only if the two genomic separations are not more than 50% different. Distances were classified according to the set of measurements (EE in red, LL in blue and LE in green) and sorted from the smallest to the largest genomic separation. A logarithmic colormap was used for the p-values.



**Supplementary Figure S11: Replication domains correspond to structural self-interacting domains.** Hi-C proximity heat-map for the intra-chromosomal interactions in Gm06990 cells on the chr5:150-175Mb locus. Each pixel represents the interaction in a 100 kb window. The colormap represents the number of reads for every pixel. A replication domain delimited by two local timing peaks corresponds to a self-interacting domain in Hi-C data, indicating that the timing peaks delineate the frontiers of megabase-sized structural domains. The CTCF track corresponds to the RAW signal of CTCF binding site in Gm06990 cells resampled at 40 kb (mean from wgEncodeUwTfbsGm06990CtcfStdRawRep1 table). Many post-translational modifications of histones and other chromatin features also correlate with the replication timing in mammals (3, 4) making unlikely, with only 5 structural domains, to identify the key chromatin factors specifying the boundaries.

Name	Chromosome 5 annealing sequence
P1_Hind	GAGGTTTCAGAGTTCAAGAAAGCTT
P1_Hin1II	GTACCTCGCTGGTGAAAACATG
P2_Hind	CCTCAGTCCTTTAAAGTGAAGCTT
P2_Hin1II	CAAGCACAACCACCAAGAACATG
P3_Hind	ATCACTTTATGTAGCAGTGAAGCTT
P3_Hin1II	GCATTATTAATAAGTTTCCACCATG
P4_Hind	AAGAGAAACGGATTGTTATGAAAGCTT
P4_Hin1II	TGGGTTACTATGTAAGGCCTCC
P5_Hind	GAGGAAAGAGAAGAATGAGTGCATG
P5_Hin1II	CCCCTGACCTTCCCAGAAGCTT
S_Hind	TTAACTTGGTGAATAAATCAGAAGCTT
S_Hin1II	TCAAATAAGGACTCTGGCAGTTG
V1_Hind	GGCAACTTTTAGTTCAATTCAAAAGCTT
V1_Hin1II	GAACAATGTCCCATCCATTCTAG
V2_Hind	GCTGGGCTCAGGTGAAAGCTT
V2_Hin1II	CAATGGAGCCACTGATTACACATG
V3_Hind	TTTGAGGGGATTATCAAGAAAGCTT
V3_Hin1II	GGTACAGATGATATGAAAATCATTAAAC
V4_Hind	TTATAATAAAAGGCAGAAAGGAAGCTT
V4_Hin1II	CAATGACCTCTACTGCAAATCATG

**Supplementary Table S1: Primers used for the 4C-Seq experiment.** Similar strategy than in (5) was employed: we used primers containing in 5' the adaptor required for Solexa sequencing and in 3' the chromosome annealing sequence. Primers were paged purified before the PCRs. The annealing sequence is shown in this table.

hg18_Start	hg18_End	name
153,892,419	154,043,563	<b>CTD-2568P10</b>
155,277,598	155,458,580	<b>RP11-484D20</b>
156,685,117	156,887,519	<b>RP11-152N9</b>
159,722,795	159,901,802	<b>RP11-135K8</b>
161,669,550	161,831,097	<b>RP11-587H15</b>
162,035,265	162,156,312	<b>CTD-3080G20</b>
162,736,912	162,903,669	<b>RP11-1012</b>
163,714,926	163,854,439	<b>RP11-1122J9</b>
165,164,376	165,335,162	<b>CTD-3159G23</b>
165,994,779	166,159,481	<b>RP11-669E20</b>
167,614,694	167,782,307	<b>RP11-277P14</b>
168,278,178	168,401,684	<b>CTD-3188O5</b>
168,909,434	169,092,364	<b>RP11-486H5</b>

**Supplementary Table S2: BAC clones used for the FISH experiments.** BAC Clones were purchased from Life Technology. Their specificity was tested by restriction analysis and hybridization localization on metaphase spreads before any distance measurement.

<b>Viewpoints</b>	<b>P1</b>	<b>P2</b>	<b>P3</b>	<b>P4</b>	<b>P5</b>	<b>S</b>	<b>V1</b>	<b>V2</b>	<b>V3</b>	<b>V4</b>	
Reads number (absolute)											(total)
Lymphoblastoid	2 740 247	2 719 730	2 070 107	2 733 911	3 589 694	2 841 857	2 955 540	2 891 073	2 075 915	1 766 323	<b>26 384 397</b>
PHA Lympho	2 541 407	8 127 305	1 994 584	10 781 467	14 167 304	7 523 709	8 069 640	12 079 074	6 568 336	7 893 763	<b>79 746 589</b>
Resting Lympho	6 890 248	6 015 350	5 603 514	8 071 340	11 488 271	7 601 659	6 857 206	8 646 373	5 617 122	6 153 403	<b>72 944 486</b>
Interval (in Mb) around the viewpoint containing 75% of chromosome 5 reads											(mean)
Lymphoblastoid	4,91	2,83	3,13	5,65	3,93	2,43	3,58	2,67	2,65	2,5	<b>3,428</b>
PHA Lympho	5,16	0,945	4,11	6,02	2,4	1,67	2,12	2,18	2,78	2,39	<b>2,9775</b>
Resting Lympho	7,72	1,56	6,57	11,01	7,14	5,09	4,53	4,54	6,17	5,9	<b>6,023</b>

**Supplementary Table S3: Read number and distribution.** 4C-Seq reads were first processed to identify the viewpoints and then mapped on the human genome (UCSC hg18 assembly). This table summarizes the number of reads identified for every cell line and viewpoint. In addition, we provide the size of the interval centered on the viewpoint containing 75% of the whole chromosome 5 reads. This interval is a few Mb, confirming that most of the interactions captured are local interactions. Reads corresponding to non-digested product were not included for the calculation of the 75%-interval. The 4C-Seq PCR corresponding to PBMC have been sequenced on Solexa Hi-Seq 2000, whereas the ones from lymphoblastoid cells have been sequenced on Solexa Genome Analyzer IIx. This explains the difference in the number of reads for every cell types. Nevertheless, the number of different partners identified for every viewpoints of the three cell types are similar, and quite independent of the reads number (not shown).



Viewpoints	chr1	chr2	chr3	chr4	chr5	chr6	chr7	chr8	chr9	chr10	chr11	chr12	chr13	chr14	chr15	chr16	chr17	chr18	chr19	chr20	chr21	chr22	chrX
<b>Resting PBMC</b>																							
V1	1,56%	1,74%	1,65%	2,07%	80,46%	1,42%	1,17%	1,20%	0,96%	0,95%	0,96%	1,18%	1,00%	0,66%	0,44%	0,36%	0,33%	0,67%	0,13%	0,29%	0,19%	0,07%	0,55%
V2	1,63%	1,97%	1,76%	1,90%	79,40%	1,36%	1,28%	1,25%	0,99%	1,06%	1,04%	1,28%	0,93%	0,75%	0,59%	0,44%	0,39%	0,68%	0,12%	0,37%	0,21%	0,08%	0,50%
V3	1,69%	1,99%	1,72%	2,04%	79,01%	1,45%	1,38%	1,41%	1,02%	1,01%	1,13%	1,24%	1,02%	0,72%	0,45%	0,40%	0,29%	0,74%	0,15%	0,27%	0,20%	0,07%	0,61%
V4	1,70%	1,98%	1,56%	1,92%	79,75%	1,44%	1,30%	1,32%	1,01%	1,05%	1,06%	1,22%	0,94%	0,63%	0,45%	0,39%	0,28%	0,75%	0,12%	0,30%	0,19%	0,06%	0,55%
S	1,74%	2,02%	1,76%	1,92%	78,33%	1,58%	1,34%	1,34%	1,06%	1,02%	1,14%	1,34%	1,02%	0,73%	0,61%	0,49%	0,48%	0,63%	0,14%	0,38%	0,24%	0,10%	0,60%
P5	1,79%	2,05%	1,65%	1,70%	78,81%	1,34%	1,20%	1,19%	1,11%	1,20%	1,21%	1,38%	0,76%	0,74%	0,66%	0,63%	0,45%	0,77%	0,15%	0,47%	0,18%	0,06%	0,49%
P4	2,53%	2,65%	2,13%	1,99%	73,71%	1,86%	1,59%	1,65%	1,29%	1,53%	1,39%	1,65%	0,93%	0,87%	0,71%	0,58%	0,53%	0,76%	0,23%	0,44%	0,27%	0,09%	0,63%
P3	1,67%	1,83%	1,55%	1,55%	81,05%	1,25%	1,16%	1,21%	0,95%	1,05%	1,06%	1,18%	0,85%	0,62%	0,53%	0,41%	0,32%	0,59%	0,14%	0,30%	0,19%	0,06%	0,47%
P2	1,93%	1,91%	1,59%	1,47%	79,93%	1,32%	1,12%	1,17%	0,98%	1,11%	0,95%	1,27%	0,82%	0,75%	0,62%	0,45%	0,62%	0,51%	0,21%	0,38%	0,22%	0,15%	0,49%
P1	2,17%	2,19%	1,92%	1,89%	75,30%	1,80%	1,51%	1,40%	1,21%	1,41%	1,33%	1,60%	0,95%	0,89%	0,73%	0,56%	0,71%	0,70%	0,25%	0,48%	0,27%	0,15%	0,59%
<b>PHA stimulated PBMC</b>																							
V1	1,43%	1,56%	1,35%	1,54%	84,26%	1,13%	0,95%	0,92%	0,68%	0,82%	0,73%	0,85%	0,72%	0,57%	0,43%	0,32%	0,31%	0,45%	0,11%	0,22%	0,12%	0,09%	0,44%
V2	1,56%	1,65%	1,47%	1,49%	82,35%	1,37%	0,96%	1,07%	0,82%	0,94%	0,81%	0,95%	0,88%	0,67%	0,49%	0,40%	0,43%	0,49%	0,18%	0,30%	0,15%	0,15%	0,44%
V3	1,54%	1,82%	1,56%	1,58%	82,35%	1,29%	1,11%	1,03%	0,88%	0,87%	0,82%	0,93%	0,84%	0,59%	0,48%	0,34%	0,29%	0,53%	0,13%	0,26%	0,16%	0,11%	0,50%
V4	1,40%	1,70%	1,45%	1,56%	83,34%	1,20%	1,01%	1,05%	0,81%	0,87%	0,81%	0,83%	0,70%	0,59%	0,43%	0,37%	0,29%	0,47%	0,17%	0,22%	0,15%	0,08%	0,48%
S	1,84%	1,76%	1,48%	1,55%	81,98%	1,27%	1,11%	1,04%	0,77%	0,87%	0,84%	0,98%	0,86%	0,66%	0,51%	0,33%	0,37%	0,49%	0,16%	0,34%	0,19%	0,13%	0,45%
P5	1,61%	1,80%	1,29%	1,39%	83,30%	1,19%	1,01%	0,93%	0,78%	0,91%	0,83%	1,05%	0,78%	0,55%	0,54%	0,24%	0,34%	0,46%	0,13%	0,29%	0,12%	0,08%	0,40%
P4	2,04%	2,12%	1,61%	1,40%	80,33%	1,66%	1,23%	1,17%	0,87%	1,04%	0,94%	0,95%	0,72%	0,66%	0,69%	0,35%	0,37%	0,56%	0,17%	0,32%	0,18%	0,10%	0,52%
P3	1,67%	1,87%	1,42%	1,47%	82,54%	1,39%	1,13%	1,08%	0,71%	0,88%	0,89%	0,93%	0,78%	0,54%	0,57%	0,32%	0,29%	0,43%	0,12%	0,25%	0,15%	0,09%	0,47%
P2	2,28%	2,02%	1,71%	1,48%	79,62%	1,54%	1,13%	1,12%	0,89%	1,07%	0,96%	1,10%	0,83%	0,72%	0,72%	0,41%	0,55%	0,42%	0,23%	0,33%	0,17%	0,19%	0,51%
P1	2,35%	2,19%	1,92%	1,66%	76,98%	1,81%	1,42%	1,26%	1,03%	1,10%	0,98%	1,27%	0,94%	0,91%	0,75%	0,48%	0,66%	0,55%	0,26%	0,45%	0,21%	0,20%	0,62%
<b>Lymphoblastoids</b>																							
V1	1,92%	2,19%	1,91%	1,94%	77,80%	1,65%	1,34%	1,41%	1,03%	1,02%	1,20%	1,12%	1,11%	0,79%	0,61%	0,40%	0,41%	0,70%	0,20%	0,32%	0,20%	0,12%	0,60%
V2	2,37%	2,42%	1,96%	1,88%	76,39%	1,88%	1,59%	1,37%	0,97%	1,20%	1,33%	1,16%	0,86%	0,92%	0,64%	0,49%	0,57%	0,55%	0,20%	0,39%	0,16%	0,14%	0,56%
V3	2,09%	2,70%	2,12%	2,21%	75,49%	1,96%	1,63%	1,49%	1,01%	1,18%	1,23%	1,31%	1,02%	0,75%	0,60%	0,48%	0,40%	0,75%	0,11%	0,37%	0,24%	0,09%	0,76%
V4	1,82%	2,21%	1,73%	1,91%	78,88%	1,62%	1,48%	1,38%	0,86%	1,10%	1,15%	1,01%	0,92%	0,71%	0,53%	0,35%	0,35%	0,62%	0,16%	0,27%	0,20%	0,08%	0,64%
S	2,31%	2,33%	1,97%	1,81%	76,46%	1,58%	1,41%	1,39%	1,03%	1,29%	1,32%	1,25%	1,04%	0,84%	0,68%	0,53%	0,58%	0,64%	0,18%	0,40%	0,23%	0,18%	0,56%
P5	2,03%	2,09%	1,80%	1,77%	78,70%	1,51%	1,25%	1,34%	1,04%	1,24%	1,40%	0,94%	0,79%	0,83%	0,65%	0,41%	0,35%	0,58%	0,16%	0,33%	0,18%	0,09%	0,52%
P4	2,37%	2,82%	2,16%	2,04%	74,39%	2,09%	1,65%	1,57%	1,04%	1,35%	1,32%	1,35%	0,92%	0,82%	0,78%	0,48%	0,52%	0,73%	0,26%	0,36%	0,22%	0,09%	0,67%
P3	1,88%	2,24%	1,80%	1,84%	79,40%	1,60%	1,31%	1,25%	0,89%	0,96%	1,10%	1,08%	0,88%	0,68%	0,57%	0,37%	0,40%	0,58%	0,10%	0,27%	0,15%	0,07%	0,56%
P2	2,12%	2,25%	1,89%	1,62%	76,98%	1,90%	1,43%	1,33%	1,15%	1,15%	1,18%	1,27%	0,90%	0,85%	0,75%	0,42%	0,52%	0,69%	0,20%	0,45%	0,19%	0,17%	0,62%
P1	3,10%	3,22%	2,50%	2,20%	69,33%	2,22%	1,79%	1,71%	1,36%	1,51%	1,68%	1,72%	1,22%	1,06%	0,91%	0,74%	0,83%	0,85%	0,30%	0,55%	0,29%	0,21%	0,72%

**Supplementary Table S4: Proportion of reads per chromosome.** The reads were counted on every chromosome. In this table, the percentage of reads mapped on every chromosome is reported for every cell line and every viewpoint. At least 70% of the reads are localized on the chromosome 5.

## References

- [1] Hansen, R. S., Thomas, S., Sandstrom, R., Canfield, T. K., Thurman, R. E., Weaver, M., Dorschner, M. O., Gartler, S. M., and Stamatoyannopoulos, J. A. (2010) Sequencing newly replicated DNA reveals widespread plasticity in human replication timing. *Proc Natl Acad Sci U S A*, **107**, 139–144.
- [2] Chen, C.-L., Rappailles, A., Duquenne, L., Huvet, M., Guilbaud, G., Farinelli, L., Audit, B., d'Aubenton-Carafa, Y., Arneodo, A., Hyrien, O., and Thermes, C. (2010) Impact of replication timing on non-CpG and CpG substitution rates in mammalian genomes. *Genome Res*, **20**, 447–457.
- [3] Hiratani, I., Ryba, T., Itoh, M., Yokochi, T., Schwaiger, M., Chang, C.-W., Lyou, Y., Townes, T. M., Schübeler, D., and Gilbert, D. M. (2008) Global reorganization of replication domains during embryonic stem cell differentiation. *PLoS Biol*, **6**, e245.
- [4] Ryba, T., Hiratani, I., Lu, J., Itoh, M., Kulik, M., Zhang, J., Schulz, T. C., Robins, A. J., Dalton, S., and Gilbert, D. M. (2010) Evolutionarily conserved replication timing profiles predict long-range chromatin interactions and distinguish closely related cell types. *Genome Res*, **20**, 761–770.
- [5] Splinter, E., de Wit, E., Nora, E. P., Klous, P., van de Werken, H. J. G., Zhu, Y., Kaaij, L. J. T., van Ijcken, W., Gribnau, J., Heard, E., and de Laat, W. (2011) The inactive X chromosome adopts a unique three-dimensional conformation that is dependent on Xist RNA. *Genes Dev*, **25**, 1371–1383.